USGS
science for a changing world

Prepared for the National Aeronautics and Space Administration

Geologic Map of the Lada Terra Quadrangle (V–56), Venus

By P. Senthil Kumar and James W. Head

Pamplet to accompany
Scientific Investigations Map 3249

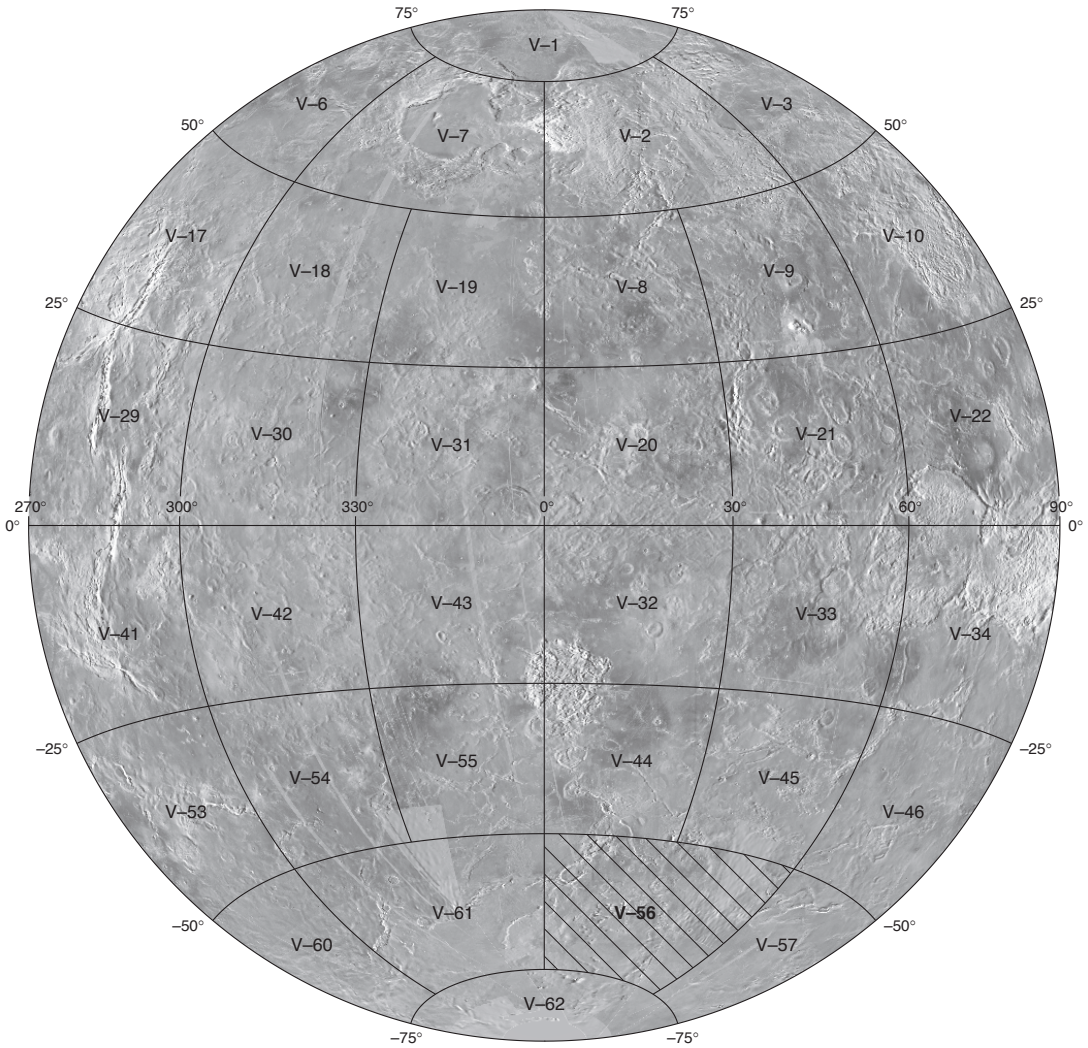

2013

U.S. Department of the Interior
U.S. Geological Survey

Contents

Introduction....1
Magellan SAR Data and Analysis....1
General Geology....2
Map Units....3
- Heavily Deformed Terrain Material....3
  - Tessera Terrain Material....3
  - Tessera-like Terrain Material....3
  - Densely Lineated Terrain Material....4
- Regional Plains Material....4
  - Wrinkle Ridged Plains Material....4
  - Regional Plains Material....4
- Volcanogenic Plains Material....4
  - Shield Plains Material....4
  - Intra-tessera Basin Plains Material....5
  - Lobate Plains Material....5
- Impact Crater Material....5

Structures....5
- Primary Structures....5
  - Shields....5
  - Channels....5
  - Lobate Flow Fronts....6
  - Impact Crater Rim....6
- Secondary Structures....6
  - Lineaments....6
  - Fractures....6
  - Faults....6
  - Grabens....6
  - Linear Ridges....6
  - Wrinkle Ridges....6

Stratigraphic Relations....7
Geologic History....8
Summary....8
Acknowledgments....9
References Cited....9

Table

1. Morphology of impact craters in Lada Terra quadrangle (V–56), Venus....11

Geologic Map of the Lada Terra Quadrangle (V–56), Venus

By P. Senthil Kumar[1,2] and James W. Head[2]

Introduction

Geologic mapping provides fundamental information on the distribution of material units and structural geologic features on a planetary surface and establishes age relations among these units. By understanding the petrogenesis of mapped material units and the tectonic history from the deformational structures, the geologic map provides significant insight into the processes of crustal evolution. On Earth, geologists prepare geologic maps in various spatial scales by carrying out field geologic analyses, whereas orbiter images are extensively used in preparing global or local geologic maps of other planetary surfaces. On Venus, although previous missions such as Venera 15/16 and Arecibo Earth-based radar observations showed a variety of surface geologic features, the Magellan mission provided a global coverage of radar images (~98%), and these images were used in preparing a global geologic map (Ivanov and Head, 2011).

This publication provides a geological map of Lada Terra quadrangle (V–56), a portion of the southern hemisphere of Venus that extends from lat 50° S. to 70° S. and from long 0° E. to 60° E. V–56 is bordered by Kaiwan Fluctus (V–44) (Bridges and McGill, 2002) and Agnesi (V–45) quadrangles in the north and by Mylitta Fluctus (V–61) (Ivanov and Head, 2006), Fredegonde (V–57) (Ivanov and Head, 2010a), and Hurston (V–62) quadrangles in the west, east, and south, respectively. The geological map of V–56 quadrangle reveals evidence for tectonic, volcanic, and impact processes in Lada Terra in the form of tesserae, regional extensional belts, coronae, and volcanic plains. In addition, the map also shows relative age relations such as overlapping or cross-cutting relations between the mapped geologic units. The geology observed within this quadrangle addresses (1) how coronae evolved in association with regional extensional belts and (2) how tesserae, regional plains, and impact craters, which are also significant geological units observed in Lada Terra quadrangle, were formed.

Several previous works have addressed the formation mechanisms and relations observed between coronae and regional extensional belts within Lada Terra quadrangle. One important previous work pertaining to Lada Terra quadrangle is by Baer and others (1994), who observed overlapping age relations between the coronae and extensional belts and suggested an inter-linked origin. The studies by Magee and Head (1994, 1995) and Schubert and Sandwell (1995) discussed the mantle processes relating to the convergence and divergence in Lavinia Planitia, Lada Terra, and Derceto Corona. Lopez and others (1999) found similarities between the coronae-extensional belts in Lada Terra and the East African rift system on Earth. Stofan and others (1992) studied the morpho-structural characteristics of some of the coronae (Quetzalpetlatl, Eithinoha, and Sarpanitum) in Lada Terra and suggested the mechanism of coronae formation related to the mantle plumes. Kratter and others (2007) studied the Arecibo radar images of Quetzalpetlatl Corona and surrounding regions and identified several pahohae lava flows emanating from Quetzalpetlatl Corona and a few new impact craters. Based on a detailed geological mapping and topographic analysis, Ivanov and Head (2010b) showed that Lada Terra rise and Quetzalpetlatl Corona form a region of long-lived mantle upwelling and recent volcanic activity. Although the above studies provided many insights to the material units and structural features and the attendant geologic processes in Lada Terra, this publication provides a geologic map of the entire Lada Terra (V–56) quadrangle and reconstructs the geologic history within the quadrangle.

Magellan SAR Data and Analysis

The orbiting phase of the Magellan mission extended from August 10, 1990, to October 12, 1994. During mission cycles 1, 2, and 3 from September 1990 to September 1992, the spacecraft collected synthetic aperture radar (SAR) images, passive microwave thermal emissions, and measurements of backscatter power at small angle of incidence, covering ~98 percent of the surface of Venus. During mission cycles 4, 5, and 6 from September 1992 and October 1994, high-resolution gravity measurements were made. The SAR instrument operated at a wavelength of 12.6 cm (S-band) with horizontal transmit/receive polarization that allowed cloud penetration and discrimination of wavelength-scale surface roughness. The catalogue of SAR image data and image interpretation methods are provided by Wall and others (1995) and Ford and others (1993), respectively, in addition to compilations made by various other researchers.

Geological mapping of Venus has been undertaken at a wide variety of scales and by a large number of individuals, including broad terrain maps derived from Earth-based radar images (Campbell and others, 1991), classifications and geologic mapping based on Pioneer-Venus topography (Masursky and others, 1980) and imaging (Senske, 1990), comprehensive geological mapping based on the northern area covered by

[1]National Geophysical Research Institute, Council of Scientific and Industrial Research

[2]Department of Geological Sciences, Brown University

Venera-15/16 radar and altimetry data (Barsukov and others, 1986), specific thematic areas using all available data sets (Ivanov and Head, 2010b), generalized global terrain maps compiled using Magellan data (Tanaka and others, 1997; Ivanov and Head, 2011), and specific areas (quadrangles) mapped at specific scales. An example of the latter is the currently ongoing NASA program administered by the U.S. Geological Survey that involves many individual geologists and their co-workers. These NASA/USGS mapping efforts have resulted in publication of more than half of 62 1:5,000,000-scale quadrangles that cover about 45 percent of the surface of Venus. These maps provide valuable documentation of the local to regional geological settings and processes. Although there are general guidelines and conventions for geological mapping (Tanaka, 1994), the goal of compilation of these individual maps is to study specific geologic problems and processes. Therefore, individual maps often employ different guidelines and conventions in terms of the details of unit definition and mapping. For example, a worker mapping a quadrangle to study the volcanic history of a region might map individual lava flows emanating from different volcanic sources separately (McGill, 2004), while a worker assessing rift zones and tectonics problems might lump these flows into a larger unit of volcanic origin (Basilevsky, 2008). Although this approach produces valuable results for individual areas, it often makes it difficult to compare these individual maps in adjacent areas and across the planet in order to assess the general global geological evolution of Venus.

We used 250 m/pixel Magellan SAR images to prepare the geologic map at a scale of 1:5,000,000. Wherever necessary, full-resolution (75 m/pixel) images were used to observe finer details. We used ArcGIS 10.0 software for carrying out geologic mapping, following the methods of geologic unit definition and characterization of planetary surfaces (Head and others, 1978; Wilhelms, 1990), suitably modified for the Magellan SAR image data (Tanaka, 1994; Basilevsky and Head, 2000; Ivanov and Head, 2001; Hansen, 2000). For the Magellan data, emissivity and radar reflectivity are used to characterize the geologic units based on geomorphology. Although geomorphologic maps do not necessarily represent stratigraphic rock units, they are very useful in determining the local, regional, and global distribution of features (such as ridge belts, scarps, and lobes) defining morphostratigraphic material units. Primary structures formed by material emplacement processes, such as volcanism and impact cratering, are also analyzed to infer the attendant geologic processes. Well-known primary structures include channels, shields, and lobate flow fronts. The SAR images are also useful to map the various secondary structures on the surface of Venus (Farr, 1993; Stofan and others, 1993; Solomon and others, 1992; Tanaka, 1994). Observed secondary structures include wrinkle ridges, folds, fractures, and shear zones or fault systems. These features are manifested in SAR images as lineaments and surfaces with radar brightness or darkness and tonal contrast that are used to characterize the form, position, and orientation of these structures, as well as to establish the relative age relations between them (such as cross-cutting relations).

General Geology

Geological units in V–56 quadrangle were products of tectonics, volcanism, and impact cratering showing their characteristic landforms. The surface is characterized by the lowlands and highlands; the boundary between these two lies at ~1.5 km above the mean planetary radius (fig. 1). The highlands are characterized by heavily deformed landforms such as tesserae, coronae, and large-scale extensional belts, suggesting that crustal deformation played an important role in the regional highland formation. The lowlands, in general, are plains characterized by lava-flow materials that traveled for several hundreds of kilometers. The slopes of the highlands enabled the lava flows to travel for longer distances and pond over the regional to local depressions in the lowlands. Aibarchin Planitia and Mugazo Planitia are typical examples of lowlands that are filled with volcanic materials.

Lada Terra is a broad region of midlands (0–2 km above mean planetary radius, MPR) at high southern latitudes (lat 60°–80° S.; long 300°–90° E.). Its western portion is dominated by a large (~2,000 km across) dome-shaped structure, a topographic rise whose summit reaches elevations 2.5–3 km above MPR. The vast lowland of Lavinia Planitia (1–1.5 km below MPR) surrounds the western portion of Lada Terra. Before the Magellan mission, the regional geology of Lada Terra was known on the basis of topographic data acquired by the Pioneer-Venus altimeter (Masursky and others, 1980; Pettengill and others, 1980) and radar images received by the Arecibo telescope (Campbell and others, 1991; Senske and others, 1991). Arecibo radar images and early Magellan results showed that Lada Terra is the site of numerous coronae including one of the largest coronae on Venus, Quetzalpetlatl Corona (Stofan and others, 1992), interconnected by belts of fractures and grabens (Baer and others, 1994; Magee and Head, 1995). One of these belts, Kalaipahoa Linea in V–61, extends from the east to the west along a regional break in slope in the marginal zone between Lada Terra and Lavinia Planitia. In contrast to Lada Terra, there are no coronae within Lavinia Planitia and the floor of the lowland is populated by complex patterns of deformational features in the form of ridge belts and grooves (see Ivanov and Head, 2006). Among the most spectacular morphologic features of Lada Terra are large complexes of lava flows emanating from coronae.

The most prominent tectonic features of V–56 are the traverses of four large-scale extensional belts (fig. 2) (Baer and others, 1994). These include the (1) north-northwest-trending, 6,000-km-long and 50–200-km-wide Alpha Regio-Lada Terra belt (Alpha-Lada belt), (2) north-northeast-trending, 2,000-km-long and 300-km-wide Derceto Corona-Quetzalpetlatl Corona belt (Derceto-Quetzalpetlatl belt), (3) north-south-trending Dyamenyuo Corona belt (Dyamenyuo belt), and (4) east-northeast-trending Geyaguga Chasma belt (Geyaguga belt). The latter two extensional belts form branches of the Alpha-Lada belt. Corona structures are also very abundant in this quadrangle and they occur preferentially along the extensional belts (fig. 2).

Lineaments are abundant in V–56 and are principally secondary deformation features such as fractures, faults, grabens, linear ridges, and wrinkle ridges. According to the classification of Stofan and others (1992), V–56 contains three concentric coronae (Quetzalpetlatl, Eithinoha, and Sarpantium), one double-ringed corona (Otygen), seven asymmetric coronae (for example, Derceto, Demvamvit, Toyo-uke, Dyamenyuo, and Ekhe-Burkhan), and one astra-like structure (Loo-Wit Mons). Radial and concentric fractures, faults, and grabens define the coronae. The large extensional belts are composed of fractures, grabens, and strike-slip zones. The areas between the large-scale extensional belts are occupied by other geological units, such as tessera terrain materials, tessera-like terrain materials, densely lineated terrain materials, regional and wrinkle ridged plains materials, shield plains materials, intra-tessera basin materials, lobate plains materials, and impact crater materials.

Map Units

Material units and primary and secondary structures are described on the basis of their radar brightness, roughness, morphology, and stratigraphic relations. The material units are shown as polygons filled with distinct color for each individual unit, whereas the structures are shown as points for volcanic features (for example, shields) and lines for channels and deformational structures, such as grabens, fractures, and faults. The material units are divided into three groups: heavily deformed terrain material, regional plains material, and volcanogenic plains material. The first group, the heavily deformed terrain material, is categorized based on unique deformational structures observed exclusively within these units. They constitute about 17 percent of V–56, including tessera terrain material, tessera-like terrain material, and densely lineated terrain material. The second group, the regional plains material, is characterized by relatively smooth radar surfaces, which host a variety of younger deformational structural features that also traverse the adjoining material units. Two types of plains characterize these geologic units (the regional plains materials and the wrinkle-ridged plains materials) and both constitute about 35 percent of V–56. The third group, volcanogenic plains material, is characterized by primary volcanic structures, for example, shields, channels, and lobate features. These units are also characterized by smooth surfaces that vary in small-scale surface roughness to yield a range of radar brightness with well-defined unit boundaries. They are classified into the shield plains materials, intra-tessera basin plains materials, and lobate plains materials; they are the most abundant material units in V–56, covering 48 percent of the surface area. V–56 contains 15 impact craters (table 1). Impact craters occupy only a fraction of the total surface in V–56 (~0.5%).

Heavily Deformed Terrain Material

Tessera Terrain Material

Tessera terrain materials (unit tt, fig. 3) are radar bright and high surface-roughness areas characterized by multiple orientations of lineaments (Barsukov and others, 1985; Basilevsky and others, 1986; Bindschadler and Head, 1991; Solomon and others, 1992; Hansen and Willis, 1998; Ivanov and Head, 1996). In V–56, at least two sets of lineaments are abundant: north-northwest-and east-southeast-oriented lineaments. Tightly spaced ridges and troughs generally characterize the tessera. The ridges (folds) and troughs (grabens) are the products of compression and extension, respectively. Cocomama Tessera and Lhamo Tessera are among the largest exposures of the tessera terrain materials in V–56. Tessera terrain materials occupy about 570.6 x 10^3 km^2 (8.9% of V–56 map area).

Tessera terrain material was discovered during the Venera 15/16 mission (Barsukov and others, 1985) and represents one of the most tectonically deformed types of terrain on Venus. Both the material and tectonic structures play an important role in the definition of tessera and tessera terrain material representing a classic example for the structural-material terrain unit. The material that forms the bulk of tessera is heavily deformed tectonically and the surface of the unit is characterized by at least two sets of intersecting structures, but usually several sets are visible. Tectonic features of both contractional (ridges) and extensional (grabens and fractures) origin occur at different scales, from a few hundred meters to several tens of kilometers in width and to several hundreds of kilometers in length. A diagnostic characteristic of tessera is its high radar-backscatter cross section, which is noticeably higher than that of the surroundings. The surface is rough at all scales, compared to most other units, and usually stands topographically higher than the surroundings. The tessera terrain material occupies about 7.3 percent of the mapped area (Ivanov and Head, 2011).

Tessera-like Terrain Material

The tessera-like terrain material (unit tlt, fig. 4) is also known as tessera transitional terrain material (Ivanov and Head, 2001; Basilevsky, 2008). It is radar bright and has high surface-roughness areas characterized by multiple orientations of lineaments but with wider spacing between the lineaments. The lineaments are north-northeast- to northeast-oriented ridges and troughs, which are cut by east-southeast- to northwest-oriented troughs. The spacing of these structures is greater than the structures in the tessera. In the northeastern part of the quadrangle, unit tlt is abundant. The tessera-like terrain material occupies about 315.2 x 10^3 km^2 (4.9% of V–56 map area). Unit tlt is also

found elsewhere on Venus. Ivanov and Head (2001) showed some examples of tessera-like terrain materials along the 30° N. global geo-traverse, and Basilevsky (2008) found these materials in Beta Regio (V–17) quadrangle.

Densely Lineated Terrain Material

The densely lineated terrain material (unit tdl, fig. 5) forms radar-bright areas with moderate surface roughness characterized by tightly spaced parallel lineaments (Basilevsky and Head, 2000; Ivanov and Head, 2001; Basilevsky, 2008). The characteristic pattern of deformation plays a very important role in the definition of densely lineated plains and, thus, this unit represents a typical structural-material unit. The lineaments form a near-parallel arrangement of ridges, grooves, and troughs. In most places, these units are also spatially associated with the tessera and tessera-like terrain materials, except for a few isolated exposures. The lineaments that characterize the tdl unit are also common in the adjoining tessera and tessera-like terrain materials. They occupy a small area of the global map, about 7.2 x 10^6 km^2 or 1.6 percent of the global map and are observed as slightly elevated and usually small (tens of kilometers across) occurrences (Ivanov and Head, 2011). In the majority of occurrences, the lineaments in unit tdl are packed so densely that they completely obscure the morphology of the precursor materials. Unit tdl occupies about 168.3 x 10^3 km^2 (2.6% of the mapped area) in V–56.

Regional Plains Material

Wrinkle Ridged Plains Material

The wrinkle ridged plains material (unit pwr, fig. 6) is plains material containing dense concentrations of wrinkle ridges (McGill, 1993; Bilotti and Suppe, 1999). Large exposures of unit pwr are seen in Aibarchin Planitia, Mugazo Planitia, and Kaiwan Fluctus regions. The wrinkle ridges, in general, occur only in the plains material. Unit pwr constitutes about 365.5 x 10^3 km^2 or 5.7 percent of V–56.

Regional Plains Material

The regional plains material (unit pr, fig. 7) occurs extensively in V–56 and is characterized by a smooth surface on radar images with varying radar brightness. Regional plains are defined by the characteristic morphology of their material and, thus, belong to the class of true material units. The unit is interpreted to be regional plains of volcanic origin. Volcanic edifices and sources of the plains are commonly not obvious at the resolution of Magellan data. Regional plains represent the most widespread material unit in V–56, occupying about 1,817.9 x 10^3 km^2 or 28.3 percent of V–56 compared to 40.3 percent of the map area globally (Ivanov and Head, 2011), and are composed of morphologically smooth, homogeneous plains materials of intermediate-dark to intermediate-bright radar backscatter. Materials of the plains are deformed by narrow, linear to anastomosing fractures and faults of the large-scale extensional belts and coronae. In the areas of densely occurring later deformational structures, the nature of original surface properties of the regional plains material has been substantially modified.

Volcanogenic Plains Material

Shield Plains Material

Shield plains material (units psh, pshc; figs. 5, 8) is characterized by smooth surfaces in radar images with clusters of small shields (1–20 km in diameter); the shields are circular volcanic features with illumination on the radar-looking slopes. The summit portion of many of the shields contains pits. Each shield is mapped as an individual structure (fig. 9), and shield plains are mapped as a unit when lava flows originate and surround the shields. Although shields are present in almost all material units, they are also abundant in coronae and are mapped as the shield plains corona material, unit pshc (fig. 8). Some of the shield plains in the densely lineated plains appear to be older and are mapped as shield plains material, unit psh (fig. 5).

Shield plains material is also one of the most dominant material units of Venus (for example, Basilevsky and Head, 1988, 1995; Head and others, 1992; Crumpler and Aubele, 2000; Ivanov and Head, 2001; Hansen, 2009). It covers a significant portion of the surface of Venus, about 79.3 x 10^6 km^2 or 17.4 percent of the global map (Ivanov and Head, 2011), and typically occurs as more or less equidimensional patches several tens to hundreds of kilometers across. In many cases, the shields occur close to each other and form groups of structures. The surface of both the shields and the plains surrounding them is morphologically smooth. Shield plains represent the first unit in the stratigraphic scheme that displays no pervasive deformation; unit psh is only mildly deformed by tectonic structures (wrinkle ridges and sparse fractures/grabens). Because of this, the priority in the definition of shield plains was given to the morphologic characteristics of their surface material and this unit thus represents a true material unit.

The small shields and related plains material are not completely confined to the stratigraphic interval between the heavily deformed terrain units and the regional plains (for example, the shields occurring in the densely lineated terrain materials). Some groups of small shields postdate regional plains and are associated, spatially and temporarily, with the youngest plains units (for example, the psh unit in Mugazo Planitia). The shield plains material units (psh, pshc) have a very similar morphology everywhere on Venus and occur in all published geological maps of this planet (Ivanov and Head, 2011). They constitute about 282.9 x 10^3 km^2 or 4.4 percent of the mapped area in V-56. On the other hand, unit pshc is less abundant than unit psh and occupies about 146.6 x 10^3 km^2 or 2.3 percent of V–56.

Intra-tessera Basin Plains Material

The intra-tessera basin plains material (units itbl, itbm, itbu; figs. 10, 11) is radar smooth with varying degrees of brightness and (or) darkness that fill the isolated basins occurring inside the tessera terrain materials (Ghent and Hansen, 1999; Hansen and others, 1999). This material is interpreted to be lava flows of different ages; most are derived from the units both outside and inside the tessera terrain. Stratigraphically these flows are classified into the intra-tessera basin plains lower unit material (itbl), intra-tessera basin plains middle unit material (itbm), and intra-tessera basin plains upper unit material (itbu), with decreasing age, respectively.

The intra-tessera basin plains material occurs in the form of patches within the outcrops of the tessera terrain material, which are made up of low viscosity lava flows filling the topographic lows in the tessera terrain. This plains material was recognized as "inter-tessera plains" in Pioneer Venus, Venera, and Magellan datasets (Bindschadler and others, 1992; Hansen and others, 1999). In V–56, the plains-filled basins are irregularly shaped, although some are quasi-circular, and the margins of the basins lack boundaries defining normal faults. Unit itbl constitutes about 66.2 x 10^3 km^2 or 1 percent of the mapped area. The middle unit (itbm) constitutes about 53.7 x 10^3 km^2 or 0.8 percent of the mapped area. The upper unit (itbu) is more abundant than the lower and middle units and constitutes about 117.7 x 10^3 km^2 or 1.8 percent of the mapped area in V–56.

Lobate Plains Material

Lobate plains material (units pll, plm, plu; figs. 12, 13) show dark to bright smooth surfaces on radar images and are characterized by primary structures such as lobate flow fronts (Head and others, 1992). Occurrences of the material units of the lobate plains usually have morphologically smooth surfaces that are occasionally disturbed by a few extensional features related to the rift zones. The most characteristic feature of lobate plains is their non-uniform albedo pattern consisting of numerous bright and dark flow-like features. The flows can be as long as several hundred kilometers and as wide as tens of kilometers (fig. 12). These materials are interpreted to be lava flows and are mostly derived from coronae (fig. 13). Stratigraphically, these materials are classified into lobate plains material, lower unit (pll), lobate plains material, middle unit (plm), and lobate plains materials, upper unit (plu).

Globally, the lobate plains make up a significant portion of the surface of Venus, about 37.8 x 10^6 km^2 or 8.3 percent of the global map area (Ivanov and Head, 2011). In V–56, all the lobate plains units together make up 38.7 percent of the map area, which is one of the most extensive mapped units. The lower, middle, and upper units constitute about 276 x 10^3 km^2 (4.3%), 1,303 x 10^3 km^2 (20.3%), and 908.1 x 10^3 km^2 (14.1%), respectively. Aibarchin Planitia and Mugazo Planitia are typical examples of lowlands that are filled with these volcanic materials.

Impact Crater Material

V–56 contains 15 impact craters (table 1), of which eight are complex craters, while the others are simple craters. Complex crater material is composed of ejecta material (unit ce), rim and wall material (unit cw), floor material (unit cf), and central peak material (unit cp) (fig. 14). The simple craters lack the central peak material, while containing the ejecta (unit ce), wall (unit cw), and floor (unit cf) materials similar to the complex craters. Impact craters are generally the youngest geologic units identified. The impact crater, Dinah, is cut by faults and fractures of Tsects Chasma, which is an extensional belt (fig. 15). Impact craters occupy only a fraction of the total surface in V–56 (29.5 x 10^3 km^2 or 0.5%). The impact craters, Marsh and Flagstad, depict outflow features that originate near the rim crest and flow outward, inundating the ejecta deposits (fig. 14).

Structures

Primary and secondary structures within V–56 are described here; individual structural domains are described within the regional context.

Primary Structures

The primary structures form during the emplacement of the geologic units, and their characters may assist in defining the spatial limits of individual material units. The primary structures within V–56 are shields, channels, and lobate flow fronts with flow directions.

Shields

Shields are small (<1–15 km in diameter) circular to quasi-circular features with dome, cone, shield, or flat-topped shapes that may or may not contain a central pit (Guest and others, 1992; Addington, 2001) and are interpreted as small volcanic edifices (fig. 5). We mapped shields as two groups, one with <5 km diameter and the other with >5 km. There are 5,058 shields in the <5 km category and 60 shields above 5 km diameter (fig. 9). In V–56, the shields occur in association with the shield plains material.

Channels

Channels are narrow, generally about 1 km wide, steep-sided, shallow at a scale of tens of meters, sinuous troughs morphologically similar to terrestrial fluvial channels (fig. 11), interpreted to form by channelized fluid flow (Baker and others, 1992, 1997). We mapped 17 channels in V–56. The nature of the fluid is undefined, as is the type of erosion, whether mechanical or thermal, cutting downward from the surface or upward from depth (for example, Gregg and Greeley, 1993; Bussey and others, 1995; Lang and Hansen, 2006).

Lobate Flow Fronts

Lobate flow fronts are the lobate margins of discrete lava flows (Chapman, 1999). The boundary of the lobate plains and intra-tessera basin plains is defined by the lobate flow fronts, which are easily identified in the SAR image (fig. 12). These are both bright and dark, depending upon the nature of lava flows (either pahohoe or aa flows). Flow direction, which is not a primary structure but interpreted from primary structures (for example, channels, levees, and other flow constructs), is shown as an arrow pointing in the flow direction.

Impact Crater Rim

The impact crater rim has been identified as a primary structure, because it formed during the emplacement of material units associated with the impact craters (fig. 14). The rim of a crater extends above the local surface, usually in a circular or elliptical pattern. The rim of a crater refers to the circular or elliptical ridge that raised above the pre-impact surface. In radar image, the rim appears in the form of a circular or elliptical ridge.

Secondary Structures

Secondary structures form after emplacement of the material units (for example, the structures in the heavily deformed terrain materials) and record the effects of tectonic processes; they provide clues for the operative tectonic processes (collision, rifting, uplift). In addition, the distribution and character of secondary structures may also help in the delineation of material units (for example, the boundary of the tessera terrain materials), as well as establishing temporal relations between different material units.

Lineaments

Lineaments are characterized by long and linear tectonic features, which may be fractures or fault segments that cut across the underlying material units. The lineaments shown in V–56 are specific to the tessera terrain material unit (fig. 3). There are 1,493 lineaments mapped in the tessera terrains of V–56. The lineaments appear as single straight lines or as double lines with a radar shadow juxtaposed to a radar-bright wall, indicating the presence of a trough or graben (for example, Head and others, 1991; Solomon and others, 1992; Grosfils and Head, 1994; Hansen and Willis, 1996).

Fractures

Fractures are fine, sharply defined, continuous radar-bright lineaments (figs. 7, 8) that are typically observed in the lowlands and are commonly interpreted to be fractures (Squyres and others, 1992; Basilevsky and Head, 2000). If a fracture is associated with a volcanic eruptive center, it may represent the surface expression of a subsurface dike. About 4,698 fractures have been mapped in V–56, and these are largely concentrated along the large-scale extensional belts (fig. 2).

Faults

Faults are broad, sharply defined, continuous radar lineaments (fig. 15). The faults are principally singular scarps, with radar-looking scarps brightly illuminated. Faults occur in varying morphology, including straight, curved, and branching (for example, Stofen and others, 1993; Kumar, 2005). In V–56, about 137 faults have been mapped, and most of them are associated with the fracture belts.

Grabens

Grabens are paired parallel dark and light lineaments that are separated by linear troughs (Stofan and others, 1993) (fig. 7). Grabens are the conspicuous tectonic features in V–56; there are 4,021 grabens. The majority of them have been mapped along the large-scale extensional belts and coronae. Grabens are also common in other material/terrain units such as tessera, tessera-like terrain, and densely lineated terrains. Some grabens are asymmetric basins that appear similar to sigmoidal pull-apart structures in strike-slip zones (fig. 16). In Hanghepiwi Chasma (fig. 17), the graben has a wide floor filled with lava flows. The boundaries of the chasma are ridges. On the west side, the ridges are affected by two sets of grabens: one set is oblique to the chasma boundary and the other is orthogonal. On the east side, the two sets tend to become parallel to the boundary. Around Eithinoha Corona, conjugate grabens and fractures are also present (fig. 13). Radially arranged grabens are also present in an astra-like structure, named the Loo-Wit Mons (fig. 18). Grabens are also present in the tessera terrain but these are embayed by the surrounding plains material, which restricts their presence only to the tessera. Therefore, these are shown separately as tessera grabens.

Linear Ridges

Ridges have linear topographic relief with oppositely dipping slopes (Stofen and others, 1993). The radar-looking slope is illuminated and the brightness across the crest gradually changes to darkness (fig. 19). The linear ridges are straight to curvilinear and are often associated with the coronae, for example, Otygen Corona (fig. 8) and Okhin-Tengri Corona. However, the linear ridges have also been seen in some of the densely lineated terrains and in parts of the tessera-like terrains. A prominent linear ridge belt has been noticed in Vaidilute Rupes (fig. 19) and is subparallel to Hanghepiwi Chasma (fig. 17) in the west. We mapped 834 linear ridges in V–56.

Wrinkle Ridges

Wrinkle ridges are sinuous ridges, but are less prominent compared to the linear ridges (McGill, 1993; Bilotti and Suppe, 1999). These occur widely in plains in the Kaiwan Fluctus

region (fig. 6), Aibarchin Planitia (fig. 12), and Mugazo Planitia. We mapped 450 wrinkle ridges in V–56.

Stratigraphic Relations

Contact relations of material units and secondary structures have been determined to infer the sequence of material emplacement and tectonic deformation. The materials that are in contact and not in contact have been grouped and superposition relations have been determined. The oldest known material units are the tessera terrain materials. The tightly spaced lineaments in the tessera (unit tt) are embayed by the surrounding plains materials (fig. 3). Unit tt is also in contact with unit tdl—the latter embays the former. Unit tt is cut by multiple orientations of lineaments, while unit tdl is characterized by unidirectional lineaments that are also present in the tessera. This suggests that unit tdl was emplaced after unit tt. Another material unit that shares some characteristics of the tessera is the tessera-like terrain material (unit tlt) in the northeastern quadrant of V–56 (fig. 4). Units tt and tlt are widely separated and do not have contact relations. The presence of multiple generations of lineaments with an increased spacing in unit tlt would suggest either lower strain rates compared to those in unit tt or greater compressive or tensional strength of unit tlt materials. Hence, the age of unit tlt may be the same as unit tt or slightly younger. Unit tlt is also in contact with unit tdl, and their relation is the same as that between units tt and tdl. These relations would mean that units tt, tlt, and tdl were emplaced during an intense tectonic process and that these materials were successively emplaced in a sequence of decreasing age. The heavily deformed materials also show evidence of younger tectonic deformation manifested in the form of chasma/chasmata belts (Chang-Xi, Sutkatyn, Kov-Ava, and Seo-Ne). These belts are deep, elongated, steep-sided depressions (fig. 20). The chasmata belts were formed after the emplacement of units tt, tlt, and tdl but before the formation of the surrounding plains materials.

The regional plains materials (units pwr, pr) show embayment relations with the heavily deformed terrain materials (fig. 3) and, therefore, postdate the heavily deformed terrain material and predate the volcanogenic plains material. Contacts between units pr and pwr are not exposed and, therefore, their relations are uncertain. However, the wrinkle ridges in unit pwr are absent in unit pr. If we assume that the wrinkle ridges in unit pwr were formed synchronously during a regional tectonic process (Basilevsky and Head, 2006), absence of wrinkle ridges in unit pr would indicate a younger age for unit pr. Even if the wrinke ridges were a product of a local process, then we would expect that the deformation should still affect the adjoining pre-existing materials, but there is no evidence of the wrinkle ridges affecting unit pr near the exposures of unit pwr.

After emplacement of the regional plains, the next generation of intense tectonic deformation began. For example, throughout V–56, unit pr has been affected by formation of four large-scale extensional belts and coronae structures (figs. 2, 7, 8). Formation of coronae structures is also synchronous with the formation of large-scale extensional structures. This synchronous formation is observed through complex stratigraphic relations between the coronae and extensional belts. For example, in some places the corona structures cut across the regional extensional belts (fig. 21), while in other places the latter postdate the former (fig. 13). Sarpanitum, Eithinoha, and Quetzalpetlatl Coronae puncture the Derceto-Quetzalpetlatl belt, while the Otygen, Demvamvit, and Okhin-Tengri Coronae are cut by the Alpha-Lada belt. Other coronae (Dyamenyuo and Toyo-uke Coronae, Loo-wit and Kshumay Montes) puncture two other extensional belts that branch from Alpha-Lada belt, namely Geyaguga belt and Dyamenyuo belt (fig. 2). Clearly, the coronae and extensional belts were formed after the regional plains formation and before the volcanogenic plains material. It is worth mentioning here that a portion of Alpha-Lada extensional belt must have formed after the emplacement of Dinah impact crater (fig. 15) but before Pychik impact crater.

Volcanogenic plains are the most widely spread materials in V–56, as they constitute about 48 percent of the surface. The shields responsible for the production of units psh and pshc are the most dominant volcanic primary structures observed in V–56 (fig. 9). It is uncertain whether the shields in V–56 are all of similar ages throughout V–56. However, the shield plains occurring in the heavily deformed materials (units tt, tlt, tdl) may have formed earlier. Unit pshc is present in most of the coronae that overlie unit pr and the tectonic structures present within them. Coronae also produced several lava flows that traveled several hundred kilometers across the regional plains. These lobate plains are abundant in Aibarchin Planitia, Mugazo Planitia, Astkhik Planum, and Kaiwan Fluctus areas. Contact relations show that the lava flows can be grouped into three units, pll, plm, and plu, successively from the oldest to the youngest (fig. 12). Materials comparable to the lobate plains are also present in the basins inside the tessera terrains. These intra-tessera basin materials are surrounded largely by unit tt but to a lesser extent by units tdl and psh. The tectonic structures in the surrounding units (tt, tdl, psh) predate the intra-tessera basin plains material. Because the basin plains material does not have direct contact with the regional plains material, no stratigraphic comparisons can be made between them. Units itbl, itbm, and itbu were formed by volcanism within the tessera terrains (fig. 11). However, some of the lava flows in the basins are transported through channels from the lobate plains present outside the tessera terrain. For example, some of the upper unit of lobate plains material in Ngyandu Vallis flow along a channel to the intra-tessera basin region to form the units itbm and itbu (fig. 10). This suggests that the units itbm and itbu can be correlated respectively with units plm and plu of the Ngyandu Vallis. The relation between units itbl and pll is unclear. Unit ltbl is invariably affected by a set of parallell fractures that disappear sharply along the boundary of units itbm and itbu (fig. 10), indicating the embayment of unit itbl by units itbm and itbu. Although unit itbl can be correlated with unit pll, unit itbl may be even older, because fractures in unit itbl are also common in units tt and tdl but are absent in unit pll. This uncertainty places the relative age of unit itbl over a much broader time frame and it may be older than that assigned for the unit pll.

Although a majority of deformational structures in the large-scale extensional structures and coronae were formed

after the regional plains and much before the volcanogenic plains, a small number of fractures and grabens are also present in unit pshc and the lobate plains (fig. 13). Therefore, a weak tectonic activity continued during the emplacement of these plains units or later. In addition, some fractures and grabens were also formed locally in the regional plains after the formation of the corona-extensional belt, for example, in the region east of Otygen Corona. These fractures trend in two directions: east-northeast and northwest. They appear to represent the latest deformation in the plains and could probably be related to the terrain uplift.

Impact craters are young geologic units in V–56 and are superimposed on units tt, pwr, pr, itbu, pll, and plm. Impact craters are absent in the youngest plains units, plu and itbu. Significantly, the craters in the older terrains tend to be simple craters with moderate to poor preservation. But, craters on the younger plains are complex structures with moderate to good preservation. Interestingly, in V–56, impact craters were also affected by tectonic structures. Tsects Chasma of Lada Terra extensional belt cuts across Dinah crater (fig. 15). These observations suggest that impact-cratering events may have occurred in V–56 over a long period of time, after the formation of tessera and some of the plains materials, although impacts could have occurred during the entire Venusian geologic history and may be continuing in the present.

Geologic History

The order in which the material and structural units were emplaced in V–56 provides insights into the sequence of geologic processes that formed the geologic history of this region. Geologic evolution of V–56 is divided into three periods: (1) formation of heavily deformed terrains, (2) formation of regional plains, large-scale extensional belts, and coronae, and (3) emplacement of volcanogenic plains. The processes making up the heavily deformed terrains (units tt, tlt, tdl) form the first and the earliest period of geologic activity in V–56. Tectonic features in these units suggest that the most vigorous geodynamic processes occurred in the earliest period. The observed ridges and grabens point to the repetitive occurrence of shortening and extensional processes that waned progressively over a period of time during the emplacement of units tlt and tdl. A minor volcanic activity in the form of shield eruptions and lava ponding occurred in the heavily deformed terrains after cessation of the major tectonic activity.

The second prominent period of geologic evolution involved the emplacement of regional plains materials, followed by the formation of wrinkle ridges, large-scale extensional belts, and coronae. Origin of the regional plains is unknown, because there are no associated primary volcanic structures within them. The plains emplacement event was followed by the second episode of intense tectonic activity. This tectonic episode involved the formation of large-scale extensional belts and corona (fig. 2). A complex network of grabens, fractures, and faults was formed in a wide zone of intense tectonic activity that traversed along four belts, as shown in fig. 2. Chains of corona structures were also emplaced along these extensional belts. Tectonic fabric at the Hanghepiwi Chasma and near Okhin-Tengri Corona shows involvement of strike-slip motion in the generation of the extensional belts. The coexistence of the extensional belts and coronae requires a combination of thermal processes in the sublithospheric mantle and extensional tectonics in the lithosphere leading to the break-up of the lithosphere and volcanism.

The third prominent period of geological evolution involved the emplacement of volcanogenic plains in association with the coronae emplacement. The shields are observed to have formed everywhere, most significantly around the coronae, and the lava flows that emanated from them formed the local material units. This period of shield volcanism was followed by significant volcanic eruptions around coronae that deposited large-scale lobate plains extending for several hundreds of kilometers covering almost a half of the total surface area of V–56. These volcanic plains are comparable to the large igneous provinces on Earth. Volcanic processes also occurred inside the tessera terrain, probably synchronously with the coronae volcanism, although some lava flows were transported from the exterior of the tessera materials to the interior basins. Local tectonic activities in some parts of the regional plains also occurred during the most recent period of geologic history; for example, more than six parallel fractures of several hundred kilometers length formed in Yenkhoboy Fossae, as did several tens of fractures and dikes in the region between Otygen and Ekhe-Burkhan Coronae. Impact events produced simple and complex craters in V–56. Outflow channels and deposits from the two largest craters (Flagstad and Marsh) were also observed, and their origin is consistent with the condensation of the ejecta plume producing these outflows (Sugita and Schultz, 2002), as these deposits were associated with the ejecta deposits.

The most significant geologic processes that affected V–56 and adjoining quadrangles are the formation of extensional belts and coronae and associated volcanism. Visible and Infrared Thermal Imaging Spectrometer (VIRTIS) of Venus Express has shown the Quetzalpetlatl and Otygen Coronae are associated with high thermal emissivity coinciding with some of the large lava flows (Helbert and others, 2008). The data indicate that these flows are young, probably hot lava flows (Ivanov and Head, 2010b). Magee and Head (1995) proposed the upwelling of deep mantle material as a possible source for these young basaltic lava flows. Therefore, these surface manifestations were the result of mantle upwelling (Magee and Head, 1994), operating at different spatial scales with chains of pronounced melting anomalies.

Summary

The geologic map of Lada Terra quadrangle (V–56) has been prepared at a scale of 1:5,000,000 using Magellan synthetic aperture radar images and ArcGIS. The map shows the distribution of various material units, primary and tectonic structures, and relative age relations between them. Material units are classified into (1) the heavily deformed materials such as tessera terrain, tessera-like terrain, and densely lineated

terrain materials, (2) regional plains and wrinkle ridged plains materials, and (3) volcanogenic plains materials originated from the shields and the coronae. The older geologic units such as tessera, tessera-like terrain, and densely lineated plains record an older episode of tectonic processes that operated before the emplacement of regional plains and volcanic plains. The regional plains are transected by the large-scale extensional belts, coronae, and localized fractures. The extensional belts are composed of fractures, grabens, and strike-slip zones. Interestingly, the extensional belts are also the sites of large-scale coronae formation, generating contacts that provide clear stratigraphic relations between these two units. The coronae are 50–300 km diameter, tectonic, circular domed structures, often associated with several centers of volcanism. In many places, corona structures cut across the regional extensional belts, while in other places, the extensional belts deform and thus postdate the coronae. Lava flows emanating from the coronae travel several hundred kilometers across the regional plains. Impact craters are the youngest geologic units, except for one affected by the fractures. The geologic map provides clues to the history of geodynamic processes that occurred both on the surface and in the interior of Venus. Mantle upwelling on Venus appears to operate at different spatial scales with chains of pronounced melting anomalies and is responsible for the formation of most of the material units and structural features in Lada Terra quadrangle.

Acknowledgments

Kumar acknowledges the BOYSCOST Fellowship awarded by the Department of Science and Technology (DST), Government of India; INDEX project of CSIR-NGRI; PLANEX (ISRO); Alexander Basilevsky, Mikhail Ivanov, Debra Hurwitz, Jay Dickson, Prabhat, Swarna Priya, and Rakesh Menga for productive discussions; and Director, NGRI, for permission to publish this map. Special thanks to Trent Hare at USGS for his help, which is gratefully appreciated. Technical reviews of McGowan and Roger Bannister and the suggestions from Ken Tanaka significantly improved the map.

References Cited

Addington, E.A., 2001, A stratigraphic study of small volcanoes on Venus: Icarus, v. 149, p. 16–36.

Baer, G., Schubert, G., Bindschadler, D.L., and Stofan, E.R., 1994, Spatial and temporal relations between coronae and extensional belts, northern Lada Terra, Venus: Journal of Geophysical Research, v. 99, p. 8355–8369.

Baker, V.R., Komatsu, G., Gulick, V.C., and Parker, T.J., 1997, Channels and valleys, *in* Bougher, S.W., Hunten, D.M., and Phillips, R.J., eds., Venus II: Tucson, University of Arizona Press, p. 757–793.

Baker, V.R., Komatsu, G., Parker, T.J., and 3 others, 1992, Channels and valleys on Venus—Preliminary analysis of Magellan data: Journal of Geophysical Research, v. 97, no. E8, p. 13,421–13,444.

Barsukov, V.L., Basilevsky, A.T., Burba, G.A., and 27 others, 1985, The geology and geomorphology of the Venus surface as revealed by the radar images obtained by Venera 15 and 16: Proceedings 16th Lunar and Planetary Science Conference, p. 378–398.

Barsukov, V.L., Basilevsky, A.T., Burba, G.A., and 24 others, 1986, The geology and geomorphology of the Venus surface as revealed by the radar images obtained by Veneras 15 and 16: Journal of Geophysical Research, v. 91, no. 4, p. D399–D411.

Basilevsky, A.T., 2008, Geologic map of the Beta Regio quadrangle (V–17), Venus: U.S. Geological Survey Geologic Investigations Series Map I–3023, scale 1:5,000,000.

Basilevsky, A.T., and Head, J.W., 1988, The geology of Venus: Annual Review of Earth and Planetary Sciences, v. 16, p. 295–317.

Basilevsky, A.T., and Head, J.W., 1995, Regional and global stratigraphy of Venus: A preliminary assessment and implications for the geological history of Venus: Planetary and Space Science, v. 43, p. 1523–1553.

Basilevsky, A.T., and Head, J.W., 2000, Geologic units on Venus—Evidence for their global correlation: Planetary and Space Science, v. 48, no. 1, 75–111.

Basilevsky, A., and Head, J.W., 2006, Impact craters on regional plains on Venus—Age relations with wrinkle ridges and implications for the geological evolution of Venus: Journal of Geophysical Research, v. 111, E03006.

Basilevsky, A.T., Pronin, A.A., Ronca, L.B., Kryuchkov, V.P., Sukhanov, A.L., and Markov, M.S., 1986, Styles of tectonic deformations on Venus—Analysis of Venera 15 and 16 data: Proceedings 16th Lunar and Planetary Science Conference, 399–411.

Bilotti, F., and Suppe, J., 1999, The global distribution of wrinkle ridges on Venus: Icarus, v. 139, p. 137–157.

Bindschadler, D.L., and Head, J.W., 1991, Tessera terrain, Venus—Characterization and models for origin and evolution: Journal of Geophysical Research, v. 96, no. B4, p. 5889–5907.

Bindschadler, D., Schubert, G., and Kaula, W., 1992, Coldspots and hotspots—Global tectonics and mantle dynamics of Venus: Journal of Geophysical Research, v. 97, no. E8, 13495–13532.

Bridges, N.T., and McGill, M.E., 2002, Geologic map of the Kaiwan Fluctus quadrangle (V–44), Venus: U.S. Geological Survey Scientific Investigations Series I–2747, scale 1:5,000,000.

Bussey, D.B.J., Sorenson, S.A., and Guest, J.E., 1995, Factors influencing the capability of lava to erode its substrate—Application to Venus: Journal of Geophysical Research, v. 100, no. E8, 16,941–16,948.

Campbell, D.B., Senske, D.A., Head, J.W., Hine, A.A., and Fisher, P.C., 1991, Venus southern hemisphere—Geologic characteristics and ages of major terrains in the Themis-Alpha-Lada region: Science, v. 251, p. 180–183.

Chapman, M.G., 1999, Geologic/geomorphic map of the Galindo quadrangle (V–40), Venus: U.S. Geological Survey Geologic Investigations Series I–2613.

Crumpler, L.S., and Aubele, J.C., 2000, Volcanism on Venus, *in* Sigurdsson, H., ed., Encyclopedia of volcanoes: San Diego, Academic Press, p. 727–769.

Farr, T.G., 1993, Radar interactions with geologic surfaces, *in* Ford, J.P., and 7 others, eds., Guide to Magellan image interpretation: Pasadena, CA, Jet Propulsion Laboratory and California Institute of Technology Publication 93-24, p. 45–56.

Ford, J.P., Plaut, J.J., Weitz, C.M., and 5 others, 1993, Guide to Magellan image interpretation:, Pasadena, CA, Jet Propulsion Laboratory and California Institute of Technology Publication 93-24.

Ghent, R.R., and Hansen, V.L., 1999, Structural and kinematic analysis of eastern Ovda Regio, Venus—Implications for crustal plateau formation: Icarus, v. 139, p. 116–136.

Gregg, T.K.P., and Greeley, R., 1993, Formation of venusian canali—Consideration of lava types and their thermal behaviors: Journal of Geophysical Research, v. 98, no. E6, p. 10,873–10,882.

Grosfils, E.B., and Head, J.W., 1994, Emplacement of a radiating dike swarm in western Vinmara Planitia, Venus—Interpretation of the regional stress field orientation and subsurface magmatic configuration: Earth, Moon, and Planets, v. 66, p. 153–171.

Guest, J.E., Bulmer, M.H., Aubele, J., and 6 others, 1992, Small volcanic edifices and volcanism in the plains of Venus: Journal of Geophysical Research, v. 97, p. 15949–15966.

Hansen, V.L., 2000, Geologic mapping of tectonic planets: Earth and Planetary Science Letters, v. 176, p. 527–542.

Hansen, V.L., 2009, Geologic map of the Niobe Planitia quadrangle (V–23), Venus: U.S. Geological Survey Scientific Investigations Map 3025, scale 1:5,000,000.

Hansen, V.L., and Willis, J.J., 1996, Structural analysis of a sampling of tesserae—Implications of Venus geodynamics: Icarus, v. 123, p. 296–312.

Hansen, V.L., and Willis, J.J., 1998, Ribbon terrain formation, southwestern Fortuna Tessera, Venus—Implications for lithosphere evolution: Icarus, v. 132, no. 2, p. 321–343.

Hansen, V.L., Banks, B.K., and Ghent, R.R., 1999, Tessera terrain and crustal plateaus, Venus: Geology, v. 27, p. 1071-1074.

Head, J.W., Peters, C., McCord, T.B., and 3 others, 1978, Definition and detailed characterization of lunar surface units using remote observations: Icarus, v. 33, p. 145–172.

Head, J.W., Campbell, D.B., Elachi, C.H.A.R., and 5 others, 1991, Venus volcanism—Initial analysis from Magellan Data: Science, v. 252, p. 276–288.

Head, J.W., Crumpler, L., Aubele, J., Guest, J., and Sanders, R.S., 1992, Venus volcanism—Classification of volcanic features and structures, associations, and global distribution from Magellan data: Journal of Geophysical Research, v. 97, no. E8, p. 13,153–13,197.

Helbert, J., Muller, N., Kostama, P., Marinangeli, L., Piccioni, G., and Drossart, P., 2008, Surface brightness variations seen by VIRTIS on Venus Express and implications for the evolution of the Lada Terra region, Venus: Geophysical Research Letters, v. 35, L11201, doi:10.1029/2008GL033609.

Ivanov, M.A. and Head, J.W., 1996, Tessera terrain on Venus—A survey of the global distribution, characteristics, and relation to surrounding units from Magellan data: Journal of Geophysical Research, v. 101, no. E6, p. 14,861–14,908.

Ivanov, M.A., and Head, J.W., 2001, Geology of Venus—Mapping of a global geotraverse at 30°N latitude: Journal of Geophysical Research, v. 106, no. E8, p. 17,515–17,566.

Ivanov, M.A., and Head, J.W., 2006, Geologic map of the Mylitta Fluctus quadrangle (V–61), Venus: U.S. Geological Survey Scientific Investigations Map 2920, scale 1:5,000,000.

Ivanov, M.A., and Head, J.W., 2010a, Geological map of the Fredegonade (V–57) quadrangle, Venus—Status report: Flagstaff, AZ, Abstracts of the Annual Meeting of Planetary Geologic Mappers, NASA/CP-2010-217041.

Ivanov, M.A., and Head, J.W., 2010b, The Lada Terra rise and Quetzalpetlatl Corona—A region of long-lived mantle upwelling and recent volcanic activity on Venus: Planetary and Space Science, v. 58, p. 1880–1894.

Ivanov, M.A., and Head, J.W., 2011, Global geological map of Venus: Planetary and Space Science, v. 59, p. 1559–1600.

Kratter, K.M., Carter, L.M., and Campbell, D.B., 2007, An expanded view of Lada Terra, Venus—New Arecibo radar observations of Quetzalpetlatl Corona and surrounding flows: Journal of Geophysical Research, v. 112, E04008, doi:10.1029/2006JE002722.

Kumar, P.S., 2005, An alternative kinematic interpretation of Thetis Boundary Shear Zone, Venus—Evidence for strike-slip ductile duplexes: Journal of Geophysical Research—Planets, 110, E07001, doi:10.1029/2004JE002387.

Lang, N.P., and Hansen, V.L., 2006, Venusian channel formation as a subsurface process: Journal of Geophysical Research, v. 111, E04001, doi:10.1029/2005JE002629.

Lopez, I., Marquez, A., and Oyarzun, R., 1999, Are coronae restricted to Venus?—Corona-like tectonovolcanic structures on Earth: Earth, Moon, and Planets, v. 77, p. 125–137.

Magee, K.P., and Head, J.W., 1994, A model for the origin of flood volcanism and passive rifting in the Lada Terra—Lavinia Planitia region of Venus: Lunar and Planetary Science Conference, abstract XXV, p. 821–822.

Magee, K.P., and Head, J.W., 1995, The role of rifting in the generation of melt—Implications for the origin and evolution of the Lada Terra-Lavinia Planitia region of Venus: Journal of Geophysical Research, v. 100, p. 1527–1552.

Masursky, H., Eliason, E., Ford, P.G., and 4 others, 1980, Pioneer-Venus radar results—Geology from the images and altimetry: Journal of Geophysical Research, v. 85, p. 8232–8260.

McGill, G.E., 1993, Wrinkle ridges, stress domains, and kinematics of Venusian plains: Geophysical Research Letters, v. 20, p. 2407–2410.

McGill, G.E., 2004, Geologic map of the Bereghinya Planitia quadrangle (V–8), Venus: U.S. Geological Survey Scientific Investigation Series Map I–2794.

Pettengill, G.H., Eliason, E., Ford, P.G., and 3 others, 1980, Pioneer Venus radar results, altimetry, and surface properties: Journal of Geophysical Research, v. 85, no. A13, p. 8261–8270.

Schubert, G., and Sandwell, D.T., 1995, A global survey of possible subduction sites on Venus: Icarus, v. 117, p. 173–196.
Senske, D.A., 1990, Geology of the Venus equatorial region from Pioneer Venus radar imaging: Earth, Moon, and Planets, v. 50/51, p. 305–327.
Senske, D.A., Campbell, D., Head, J.W. and 10 others, 1991, Geology and tectonics of the Themis Regio-Lavinia Planita-Alpha Regio-Lada Terra area, Venus—Results from Arecibo image data: Earth, Moon, and Planets, v. 55, p. 97–161.
Solomon, S.C., and 10 others, 1992, Venus tectonics—An overview of Magellan observations: Journal of Geophysical Research, v. 97, no. E8, 13,199–13,255.
Squyres, S.W., Jankowski, D.G., Simons, M., Solomon, S.C., Hager, B.H., and McGill, G.E., 1992, Plains tectonism on Venus—The deformation belts of Lavinia Planitia: Journal of Geophysical Research, v. 97, no. E8, p. 13,579–13,599.
Stofan, E.R., Senske, D.A., and Michaels, G., 1993, Radar interactions with geologic surfaces, *in* Ford, J.P., and 7 others, eds., Guide to Magellan Image Interpretation: Pasadena, CA, Jet Propulsion Laboratory and California Institute of Technology Publication 93-24, p. 93–108.
Stofan, E.R., Sharpton, V.L., Schubert, G., and 4 others, 1992, Global distribution and characteristics of coronae and related features on Venus—Implications for origin and relation to mantle processes: Journal of Geophysical Research, v. 97, no. E8, p. 13,347–13,378.
Sugita, S., and Schultz, P.H., 2002, Initiation of run-out flows on Venus by oblique impacts: Icarus, v. 155, p. 265–284.
Tanaka, K.L., 1994, Venus geologic mappers' handbook (2d ed.): U.S. Geological Survey Open-File Report 94-438, p. 50.
Tanaka, K.L., Senske, D.A., Price, M., and Kirk, R.L., 1997, Physiography, geologic/geomorphic mapping, and stratigraphy of Venus, *in* Bougher, S.W., Hunten, D.M., Phillips, R.J. eds.,Venus II Geology, geophysics, atmosphere, and solar wind environment: Tucson, University of Arizona Press, p. 667–694.
Wall, S.D., McConnel, S.L., Leff, C.E., and 3 others, 1995, User guide to the Magellan Synthetic Aperture Radar Images: National Aeronautics and Space Administration (NASA) Reference Publication 1356, 206 p.
Wilhelms, D.E., 1990, Geologic mapping, in Planetary Mapping: Cambridge, UK, Cambridge University Press, p. 208.

Table 1. Morphology of impact craters in Lada Terra quadrangle (V–56), Venus.

Crater name	Location (lat, long)	Diameter (km)	Structure	Preservation[1]	Target material
Akosua	18.00, –58.54	5	Simple	Weak	Tessera terrain material, wrinkle ridged plains material
Berggolts	53.00, –63.46	28	Complex	Good	Wrinkle ridged plains material, lobate plains material middle unit
Caitlin	12.00, –65.25	12	Simple	Weak	Tessera terrain material
Danute	56.50, –63.50	13	Complex	Moderate	Lobate plains material middle unit
Dinah	37.06, –62.85	16	Simple	Deformed by grabens, poor	Regional plains material
Erxleben	39.46, –50.84	33	Complex	Moderate	Tessera-like terrain material, lobate plains material middle unit
Flagstad	18.85, –54.29	40	Complex	Good, outflows in the ejecta	Regional plains material
Guilbert	13.64, –57.96	25	Complex	Moderate	Regional plains material
Hsueh Tao	12.46, –52.96	13	Simple	Weak	Tessera terrain material, regional plains material, lobate plains material middle unit
Kollado	53.36, –61.00	5	Simple	Poor	Lobate plains material middle unit
Marsh	46.62, –63.59	48	Complex	Good, outflows in the ejecta	Shield plains material
Pychik	33.77, –62.36	10	Simple	Poor	Regional plains material
Rand	59.56, –63.77	22	Complex	Moderate	Wrinkle ridged plains material
Tuyara	15.47, –62.89	12	Simple	Poor	Tessera terrain material, intra-tessera basin plains material middle unit
Von Siebold	36.71, –51.97	33	Complex	Moderate	Tessera-like terrain material, lobate plains material lower unit

[1]The preservation state of impact craters includes ejecta, rim, and crater interior.